scientific reports

Check for updates

OPEN

Multi-omics profiling reveals distinct pathogenic mechanisms in Hunner and non-Hunner interstitial cystitis subtypes

Lin Zhu[1,4], Hanwei Ke[2,3,4], Qi Wang[2,3], Kexin Xu[2,3]✉ & Xiaofang Chen[1]✉

Bladder Pain Syndrome/Interstitial Cystitis encompasses Hunner lesion and non-Hunner lesion (NHIC) subtypes, characterized by chronic pelvic pain and urinary symptoms. The two subtypes show distinct clinical presentations, yet their underlying mechanisms remain poorly understood. Advancements in biological detection technologies allow for deeper insights into disease pathogenesis through integrated multi-omics approaches. This study aims to delineate the differences between NHIC and HIC using multi-omics analysis to uncover distinct microbiome, metabolome, and transcriptome profiles, thereby elucidating their unique pathogenic mechanisms. We conducted a comprehensive analysis involving bladder tissue samples and urine specimens from NHIC and HIC patients. Genomic, metabolomic, and transcriptomic data were obtained using high-throughput sequencing techniques. Differentially expressed genes, metabolites, and microbial communities were identified and subjected to pathway enrichment analysis to explore their associations with disease subtypes. Our findings revealed significant differences in the urinary microbiota, with NHIC showing a predominance of Lactobacillus and Enterococcus, while HIC exhibited higher levels of Pseudomonas and Gardnerella. Metabolomic analysis identified altered pathways, such as arginine and proline metabolism in NHIC and steroid hormone biosynthesis in HIC. Transcriptomic profiling highlighted upregulation of immune response genes in HIC, particularly those involved in mast cell degranulation and viral infection pathways. In contrast, NHIC was associated with increased expression of metabolic and energy-related pathways. This multi-omics analysis revealed distinct pathogenic signatures between NHIC and HIC, indicating that HIC may be driven by chronic immune dysregulation and past infections, while NHIC is more closely associated with metabolic disturbances. These insights suggest potential avenues for tailored therapeutic interventions based on the molecular characteristics of each subtype. Further research is warranted to confirm these findings and explore their clinical implications.

Keywords Bladder pain syndrome, Multi-omics analysis, Microbiome, Metabolomics, Transcriptomics, Disease mechanism

Bladder Pain Syndrome/Interstitial Cystitis (BPS/IC), is a chronic inflammatory bladder condition characterized by pain or pelvic discomfort associated with a full bladder, along with lower urinary tract symptoms such as frequency or urgency[1].

In 1987, Fall et al. posited that Bladder Pain Syndrome/Interstitial Cystitis is divisible into Hunner lesion Interstitial Cystitis (HIC) and Non-Hunner lesion Interstitial Cystitis (NHIC), as they noted marked histological disparities between the two subtypes and advocated for their independent investigation[2]. For a majority of HIC patients, cauterization or excision of the Hunner ulcers yields a significant therapeutic benefit. Thus, patients afflicted with HIC who receive cystoscopy with hydrodistension exhibit superior symptom amelioration and protracted relief, as compared to those suffering from NHIC[3]. In view of the divergent clinical course of the two subtypes of BPS/IC discussed earlier, it is apparent that individualized treatment assumes primacy, underscoring the exigency to fathom the pathogenesis of both subtypes.

[1]Department of Plastic Surgery, Affiliated Beijing Chaoyang Hospital of Capital Medical University, Beijing 100020, China. [2]Department of Urology, Peking University People's Hospital, Beijing 100044, China. [3]Peking University Applied Lithotripsy Institute, Peking University People's Hospital, Beijing 100034, China. [4]Hanwei Ke and Lin Zhu equally contributed to this work. ✉email: cavinx@yeah.net; chenxiaofang2023@yeah.net

In recent years, the relentless advancement of biological detection technologies, coupled with the continuous evolution of microbiome, transcriptomics, metabolomics, proteomics, and other research methodologies, have enabled experts to unravel the molecular underpinnings of numerous intractable diseases, providing a bedrock for the implementation of individualized clinical interventions.

Isobel Walton et al. meticulously culled and statistically analyzed six studies that investigated urine microbiota profiles in healthy female controls and those afflicted with BPS/IC, yielded the following key insights: (1) Female BPS/IC patients displayed substantial inter-individual variations in urine microbiome profiles; (2) Currently, no persuasive evidence exists to support clinically significant differences in diversity or species composition between female BPS/IC and control groups; (3) Lactobacillus species emerged as the most prevalent dominant genus in both female BPS/IC and control samples; (4) Pain severity in female BPS/IC patients did not show any significant correlation with urine microbiota; (5) As of now, no promising candidate molecule or microbiome model has emerged for female BPS/IC[4].

In May 2021, J Curis Nickel spearheaded a pioneering investigation into the divergent distribution of urine microbiota in patients afflicted with HIC and NHIC, postulated that bacterial involvement in HIC pathology remained unsubstantiated, and there was no significant variation in species abundance and diversity between the two subtypes. Nevertheless, a few male samples exhibited significantly disparate abundances of Negativicoccus, Porphyromonas somalae, Mobiluncus curtisii, and Corynebacterium renale. Notably, the first two bacterial species are wound-associated anaerobic gram-negative bacteria, and the third is known to be associated with bacterial vaginosis in women. The study proposes that catheterized specimens may circumvent the limitations imposed by the interference of urethral fixed microbiota and potentially uncover subtle dissimilarities between the two subtypes[5].

A study of 42 women, comprising 20 patients with interstitial cystitis (IC) and 22 controls, implemented 16SrRNA sequencing and liquid chromatography coupled with mass spectrometry for urine microbiota and metabolite analysis. The findings indicated that the expression of four pathogenic bacterial species—Serratia, Brachybacter, Porphyromonas, and Citrate Acidobacteria—was significantly upregulated in the IC group. Additionally, alterations in IC metabolite characteristics appeared to be linked to sphingosine metabolism, amino acid metabolism, and fatty acid biosynthesis[6].

Japanese scholars have subsequently undertaken whole transcriptome sequencing on bladder biopsy specimens from non-Hunner type IC (NHIC) and Hunner type IC (HIC) patients. They discovered that HIC patients and NHIC patients displayed varying genomic and histological features, with a correlation to upregulated pathways that are involved in immune response and infection. Conversely, NHIC patients lacked these specific characteristics[7].

Despite the emergence of numerous studies on the mechanism of BPS/IC, there is still a deficiency in the exploration of multi-omics combinations such as microbiome, metabolome, transcriptome, and so forth. In our previous research on this topic, we compared the demographic and clinical characteristics of NHIC and HIC patients[8]. It can be observed that there were no statistically significant differences between the two groups in terms of age, disease duration, or voiding diaries, making it difficult to distinguish the two groups based solely on clinical symptoms. However, significant differences were observed in urodynamic and cystoscopic findings between the two groups. Therefore, this project aims to investigate the multi-omics distinctions of NHIC and HIC types, further explore the pathogenesis of the two types, and explore the correlation between clinical symptoms and molecular mechanisms of patients with different types. Ultimately, the goal is to provide a foundation for the creation of individualized treatment plans for BPS/IC patients, improve patient prognosis, and reduce patient burdens.

Results

Urine microbiome analysis

An investigation was conducted involving 18 subjects with non-Hunner type interstitial cystitis (NHIC) and 12 subjects with Hunner type interstitial cystitis (HIC). Two NHIC and five HIC subjects provided both mid-morning urine samples and intraoperative catheterization samples, resulting in a total of 37 urine samples that met sequencing quality control standards. Subsequent analysis of the microbiome was performed on these samples.

Exploring α and β diversity analysis in the MID and CATH cohorts

Initially, we performed Partial Least Squares Discriminant Analysis (PLS-DA) to classify the samples, designating the self-retained early morning mid-morning urine samples as "MID." and the intraoperative catheterization samples as "CATH." Fig. 1A visually reveals discernible distinctions between the two groups, but some samples still had close distances, with overlapping confidence ellipses, indicating no significant differences between the groups. Figure 1B–D illustrate the genus-level comparison between the two groups, examining the Chao1 index ($P=0.8983$), the Shannon index ($P=0.3067$), and the Simpson index ($P=0.4433$).For β-diversity analysis, we employed principal coordinate analysis (PCoA) and non-metric multidimensional scaling analysis (NMDS) to investigate inter-sample dissimilarities. As depicted in Fig. 1E, F, PCoA analysis did not yield a complete distinction between the two groups, with sample distances exhibiting no statistical significance ($P>0.05$). Similarly, NMDS analysis positioned the CATH group within the inner circle and the MID group in the outer circle, again with no statistically significant difference ($P>0.05$). This intriguingly suggests that the catheterization sampling method may mitigate the influence of certain miscellaneous bacteria.

Despite observing some dissimilarities in α and β diversity at the genus level, the lack of statistical significance reaffirms the earlier findings from the PLS-DA analysis. Consequently, it appears that although some variations exist between the two sampling techniques, the overall species richness and evenness remain comparatively consistent.

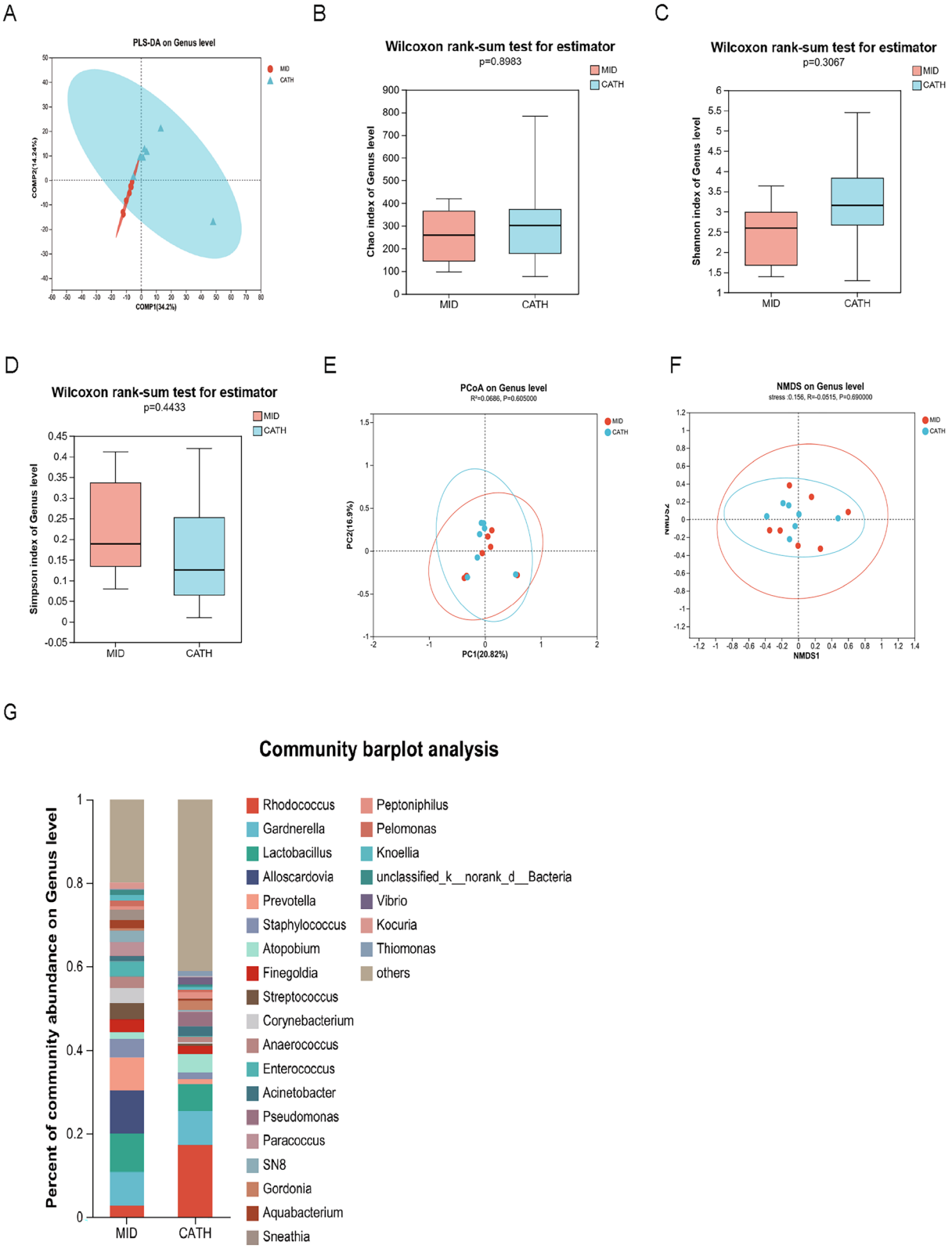

Fig. 1. Urine microbiome analysis (**A**) PLS-DA analysis at the genus level for the MID and CATH groups; (B–F) Analysis of α and β diversity in the MID and CATH groups. (**B**) Chao1 index; (**C**) Shannon index; (**D**) Simpson index; (**E**) PCoA analysis; (**F**) NMDS analysis. (**G**) Analysis of community composition in the MID and CATH groups.

Deciphering the community composition analysis of the MID and CATH cohort

Figure 1G distinctly portrays the analogous community structure of the two groups, yet accentuates the considerable dissimilarity in the relative abundance of each bacterial genus. Noteworthy disparities manifest in the MID group, where the proportion of numerous bacterial genera notably surpasses that of the CATH group.

Unveiling the species composition analysis of the NHIC and HIC cohorts

As depicted in Fig. 2A, the Venn map analysis of urine flora in the NHIC and HIC groups revealed that 852 species were shared at the genus level, with 303 species exclusive to the HIC group and 273 species unique to the NHIC group. Notably, the number of species observed in the NHIC group was slightly smaller than that in the HIC group.

Upon juxtaposing the results in Fig. S1A and Fig. S1B, a conspicuous discrepancy arises, wherein the NHIC cohort exhibits a pronounced prevalence over the HIC cohort in the proportions of Lactobacillus, Klebsiella, Enterococcus, and Prevosia. Conversely, in comparison to the NHIC group, the HIC group demonstrates a statistically significant advantage in the prevalence of Pseudomonas, Gardnerella, and Chia.

Figure 2C portrays a Circos diagram that intricately illustrates the relationship between samples and species. The small semicircle on the left depicts the species composition within each sample, with the outer ribbon color-coded to represent the corresponding group and the inner ribbon reflecting the species, with the length denoting its relative abundance. Conversely, the large semicircle on the right showcases the distribution of species among different samples at this taxonomic level. Here, the outer ribbon represents the species, the inner ribbon is color-coded to signify different groups, and the length reflects the proportion of each species in a sample. The discernible divergence in dominant urine microbiota between the two groups becomes readily apparent.

Exploring α and β diversity analysis in the NHIC and HIC cohorts

An initial PLS-DA analysis was conducted to assess sample grouping, as presented in Fig. 2B. While some differences were observed between the two groups, certain samples remained in close proximity, with overlapping regions of the confidence ellipse indicating a lack of significant difference.

The assessment of α diversity was conducted utilizing the Chao1 index, the Shannon index, and the Simpson index. As depicted in Fig. 2D, E and F, the box plot demonstrates that the NHIC group exhibited greater species richness and uniformity compared to the HIC group. However, at the genus level, there were no substantial variations between the two groups, as evidenced by the Chao1 index ($P = 0.4779$), Shannon index ($P = 0.7$), and Simpson index ($P = 0.8552$).

The PCoA and NMDS analyses are presented in Fig. 2G, H, respectively. The confidence ellipse of the PCoA analysis between the two groups exhibited a cross-overlapping segment with a *P* value greater than 0.05, although some samples showed clear differences. Similarly, the confidence ellipses of the two groups in the NMDS analysis partially overlapped, with a *P* value greater than 0.05 and a stress value lower than 0.2, indicating that the grouping model has some significance. However, there were no significant differences in β diversity between the two groups at the genus level.

Despite observing some variations in the α and β diversity at the genus level between the NHIC and HIC groups, the dissimilarities were not statistically significant, which was in line with the outcomes of the PLS-DA analysis. These findings indicate that the microbiota analysis cannot completely distinguish between NHIC and HIC subtypes, as both subtypes represent distinct presentations of BPS/IC.

Unraveling species disparities between NHIC and HIC cohorts

The LDA discriminant histogram quantified the microbial taxa in both groups, utilizing LDA analysis (a form of linear regression analysis) to obtain LDA scores. Enrichment was considered significant if the taxa exhibited *P* values less than 0.05 and LDA scores greater than or equal to 2.

Figure 2I illustrates the results of LEfSe analysis, which revealed significant differences in microbial taxa between the NHIC and HIC groups. Specifically, the Proteus genus was found to be significantly enriched in the HIC group, while the Digestive Coccus genus was significantly enriched in the NHIC group. Moreover, many common environmental bacteria, such as those found in sludge and flowers, were significantly enriched in the NHIC group.

Urine metabolomics analysis

The metabolomics study included urine samples from 17 NHIC patients and 12 HIC patients that met the quality control criteria. To eliminate the impact of urinary retention mode, all patients' urine samples were obtained through catheterization and retained.

OPLS-DA analysis of NHIC and HIC groups

OPLS-DA offers a means to assess model classification efficacy by evaluating R2X, R2Y, Q2, and OPLS-DA score maps. For this analysis, the R ropls package was employed, and the VIP (Variable Importance for the Projection) value served as a metric to gauge the significance of a variable (i.e., characteristic peak) in explaining both the X dataset and its associated Y dataset. Variables with a VIP value greater than 1 were considered important and utilized as a screening criterion for potential biomarkers.

In Fig. 3A, the NHIC and HIC samples are clearly differentiated in the positive ion mode, forming distinct clusters represented by blue and red circles, respectively. Each individual sample is depicted as a scattered small square. Notably, the ellipses of the two groups exhibit discernible differences, with the NHIC group appearing as a predominantly horizontal ellipse, and the HIC group appearing as a predominantly longitudinal ellipse with partial overlap in the middle. The R2X value is 0.408cum, while the R2Y value is 0.589cum, with a Q2 value of − 0.416cum, indicating the model's performance. Furthermore, the PR2Y value is 0.705, and PQ2 is 0.88.

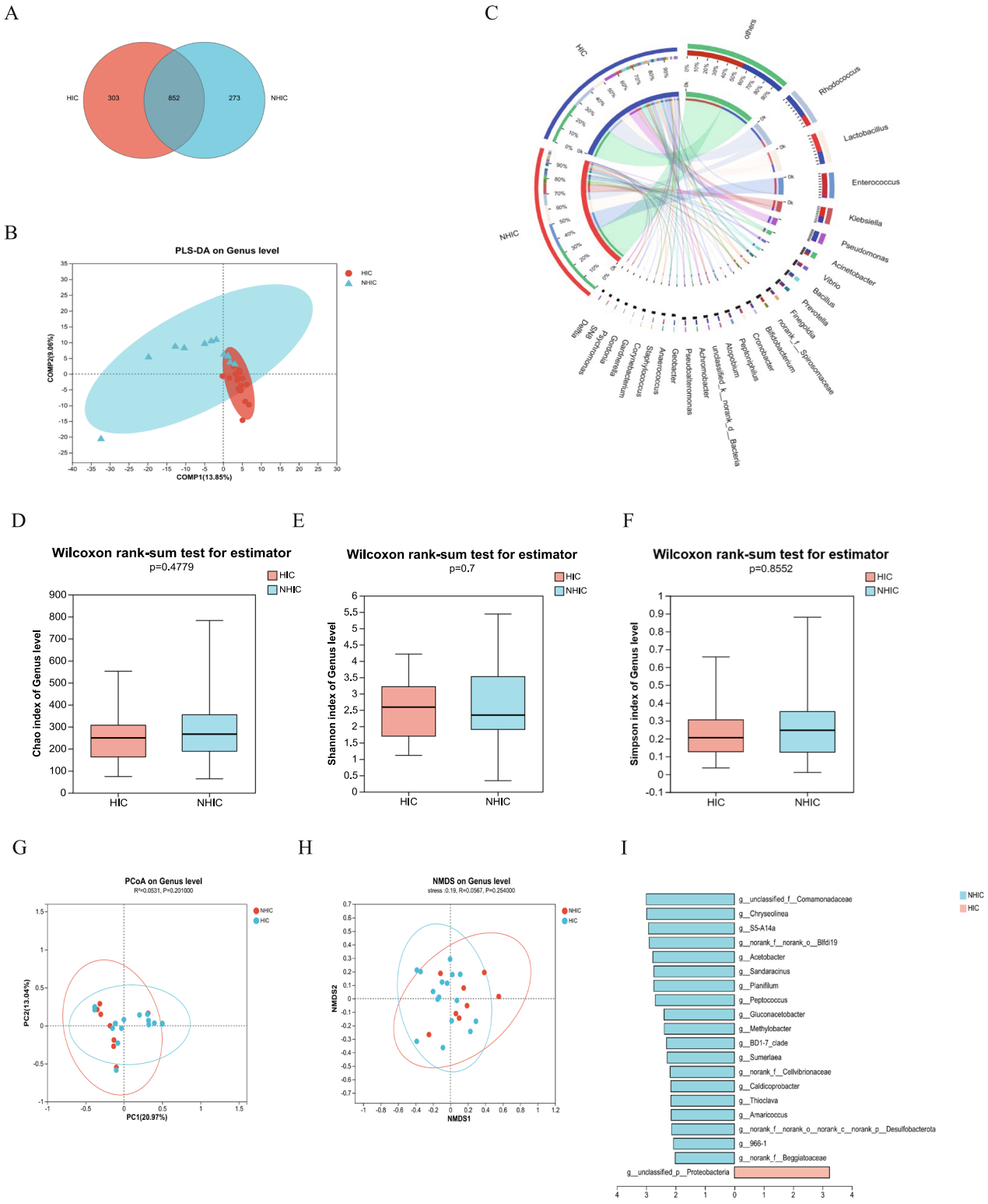

Fig. 2. Comprehensive Insights into Species Composition, α Diversity, and β Diversity in NHIC and HIC Cohorts (**A**) Venn diagram analysis of bacterial species in the NHIC and HIC microbial communities; (**B**) PLS-DA analysis at the genus level for the NHIC and HIC groups; (**C**) Distribution of dominant species in the NHIC and HIC microbial communities using a Circos plot; (**D**, **E**, **F**, **G** and **H**) Analysis of α and β diversity at the genus level in the NHIC and HIC groups;(D) Chao1 index; (E) Shannon index; (**F**) Simpson index; (**G**) PCoA analysis; (**H**) NMDS analysis.) (**I**) showcases the LEfSe analysis for discriminating species differences between the NHIC and HIC groups.

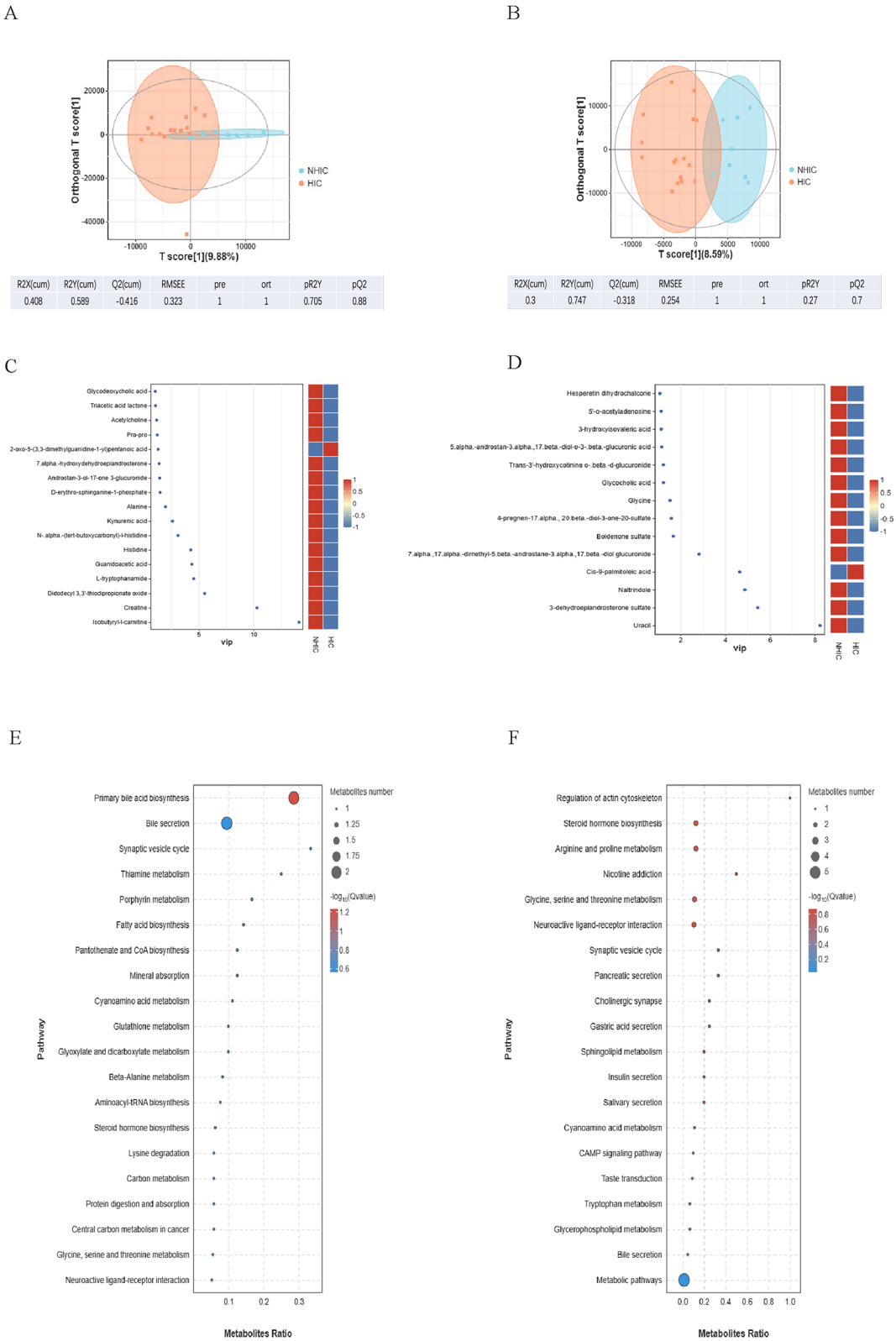

Fig. 3. Integrated Metabolomic Profiling and Pathway Enrichment Analysis Reveals Contrasts in NHIC and HIC Groups. (**A**) displays the score plot of OPLS-DA analysis in positive ion mode for the NHIC and HIC metabolomic profiles; (**B**) presents the score plot of OPLS-DA analysis in negative ion mode for the NHIC and HIC metabolomic profiles; (**C**) VIP (Variable Importance in the Projection) plot for the positive ion mode analysis of the NHIC and HIC metabolomic profiles; (**D**) VIP (Variable Importance in the Projection) plot for the negative ion mode analysis of the NHIC and HIC metabolomic profiles; (**F**) and (**E**) Bubble plot of significantly enriched KEGG pathways for differential metabolites in the NHIC and HIC groups.(**F**) Positive ion mode; (**E**) Negative ion mode).

As demonstrated in Fig. 3B, in the negative ion mode, the NHIC and HIC groups form two longitudinal ellipses with only a small overlap. The R2X value is 0.3cum, the R2Y value is 0.747cum, and the Q2 value is − 0.318cum, further assessing the model's performance. Additionally, the PR2Y value is 0.27, and PQ2 is 0.7.

Unveiling metabolic disparities: differential analysis of NHIC and HIC metabolomes
In the positive ion mode, a comprehensive differential analysis heatmap of urine metabolites between the NHIC and HIC groups is depicted in Fig. S1C. Among the extensive array of metabolites analyzed, 17 displayed statistically significant differences between the two groups. Remarkably, 16 of these metabolites exhibited down-regulated expression in the HIC group relative to the NHIC group. Singularly, one short-chain keto acid derivative displayed up-regulation in the HIC group. Figure 3C depicts the differential analysis VIP diagram, offering insight into the specific contribution of each metabolite. The abscissa represents the VIP value, while the ordinate displays the top 15 differential metabolites. We derived the mean value of metabolite abundance for each sample in each group and conducted a z-score analysis accordingly. The color on the right indicates the level of metabolite abundance in different groups, where red denotes up-regulation, and blue represents down-regulation. Notably, metabolites with VIP > 1 were deemed to exhibit significant differences.

In the negative ion mode, Fig. S1D showcases the differential metabolites, encompassing a total of 16 metabolites that exhibited remarkable differences between the NHIC and HIC groups. The VIP diagram in the negative ion mode is portrayed in Fig. 3D, shedding light on the specific contributions of the discernible metabolites.

DEMs enrichment analysis: KEGG analysis of NHIC and HIC metabolomes
In the positive ion mode, KEGG enrichment analysis was carried out on the differential metabolites between the NHIC and HIC groups. Notably, six metabolic pathways exhibited statistical significance ($P < 0.05$) between the NHIC and HIC groups, namely: arginine and proline metabolism, glycine, serine, and threonine metabolism, neuroactive ligand receptor interactions, nicotine addiction, actin cytoskeleton regulation, and steroid hormone biosynthesis, as depicted in Fig. 3E. These findings suggest the potential involvement of these metabolic pathways in the development and progression of hypertension and signify promising targets for future treatment and prevention strategies.

Similarly, in the negative ion mode, KEGG enrichment analysis was performed on the differential metabolites between the NHIC and HIC groups. Notably, primary bile acid biosynthesis, bile secretion, synaptic vesicle cycle, and vitamin B1 metabolism exhibited the most significant pathways with statistical differences ($P < 0.05$), as shown in Fig. 3F.

Transcriptomic analysis of bladder tissue

In this study, 28 HIC specimens, and 20 NHIC specimens were included in the analysis.

Principal component analysis (PCA) of transcriptomics data
To explore the global transcriptomic differences between the NHIC and HIC groups, we performed PCA on the transcriptomics dataset (Fig. 4A). The PCA plot reveals a clear separation between the two groups along the first principal component (PC1), which accounts for 75.4% of the total variance. The second principal component (PC2) explains an additional 7.6% of the variance. Samples from the NHIC group (orange) and the HIC group (blue) form distinct clusters, indicating significant transcriptional differences between the groups. Additionally, the tight clustering within each group suggests good reproducibility and minimal intra-group variation.

Decoding transcriptional disparities: differential analysis of NHIC and HIC bladder tissue transcriptomes
Transcriptome sequencing was executed on 28 HIC specimens and 20 NHIC specimens, followed by the generation of a volcano map analysis based on significantly differentially expressed genes from the two groups. In earlier studies and our previous basic studies, some BPS/IC-related potential pathogenic genes were identified. We examined the expression of these key focus genes and found that NGFR, BDNF, IL6R, IL1B, TGFBR1, ADCYAP1, CCL2, and CCL3 genes were significantly upregulated in the HIC group, whereas IL17D was downregulated significantly in the HIC group (Fig. 4B).

DEGs enrichment analysis: KEGG Analysis of NHIC and HIC bladder tissue transcriptomes
Figure 4C presents the enriched KEGG pathways in a visually informative manner. Notably, the figure illustrates 25 significantly enriched KEGG pathways, shedding light on the molecular processes underlying NHIC and HIC.

The results of this analysis demonstrate a close relationship between these significantly enriched pathways and various aspects of bacterial and viral infections, immune responses, and autoimmune diseases. These findings align with the results from the GO enrichment analysis and further emphasize the crucial role of infection and immunity in the pathogenesis of both NHIC and HIC groups.

4DEGs enrichment analysis: GO analysis of NHIC and HIC bladder tissue transcriptomes
In our GO enrichment analysis (Fig. 4D), we made significant and noteworthy discoveries regarding the differentially expressed genes between the NHIC and HIC groups. Notably, we found a substantial enrichment of 2449 entries ($P < 0.05$) in the GO biological process category, encompassing numerous terms primarily associated with immunity. These terms included immune response, immune system processes, adaptive immune response, regulation of immune system processes, cell activation, leukocyte activation, immune response regulation, response to stimuli, inflammatory response, and others, highlighting the pivotal role of immune-related processes in the pathogenesis of both groups.

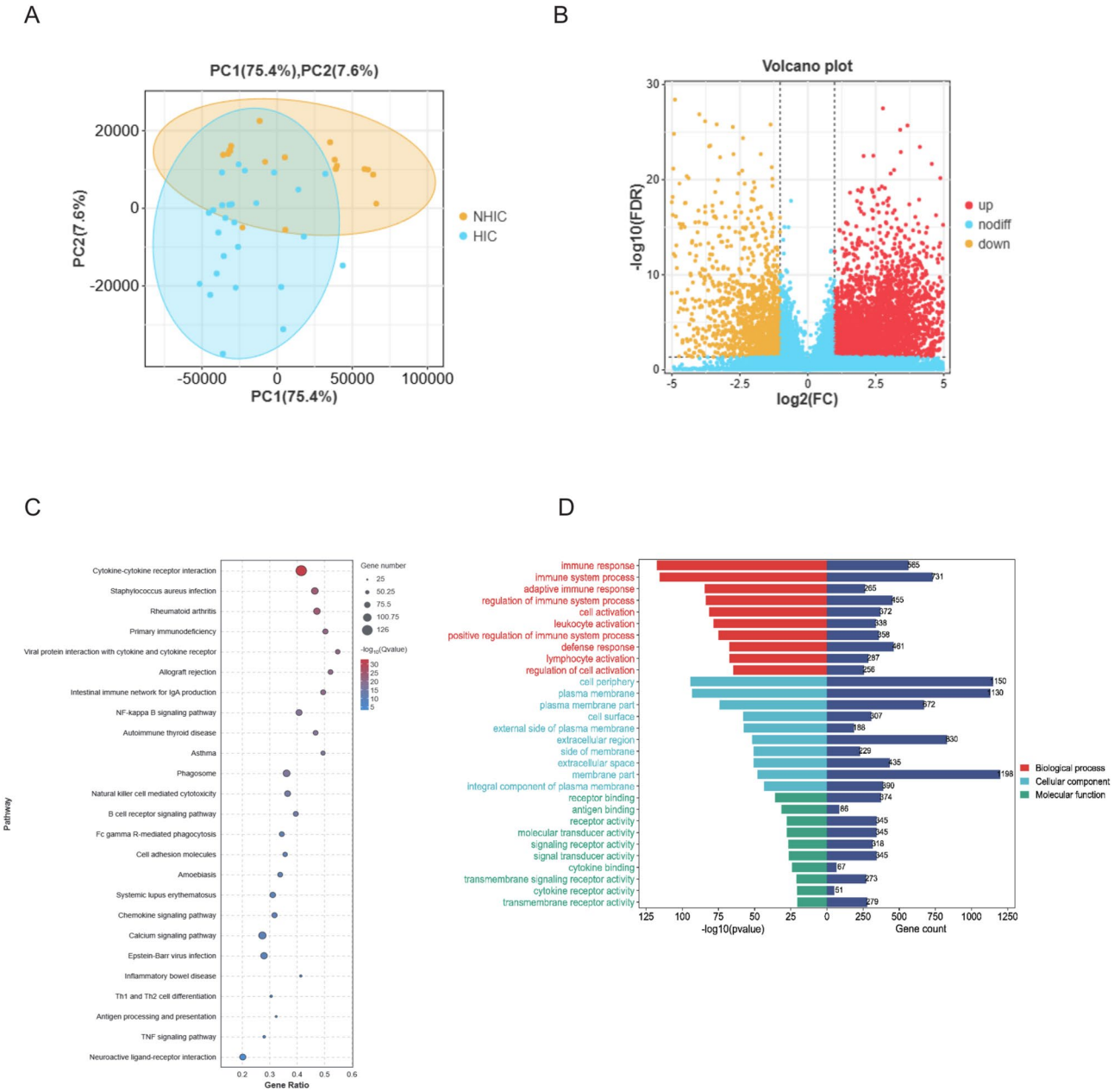

Fig. 4. Transcriptomic analysis of bladder tissue (**A**) PCA plot showing distinct clustering between the two groups, indicating transcriptional differences and good reproducibility within each group. (**B**) Volcano plot of differential gene expression analysis between the NHIC and HIC transcriptomic profiles; (**C**) KEGG enrichment analysis of the NHIC and HIC transcriptomic profiles. (**D**) GO (Gene Ontology) enrichment analysis of the NHIC and HIC transcriptomic profiles;

Furthermore, the GO molecular function analysis revealed the significant enrichment of 356 entries ($P < 0.05$), which were closely associated with receptors, ligands, cytokines, and various other molecules involved in immune activity, cell signal transduction, and virus-host interactions. Terms such as receptor binding, antigen binding, cytokine binding, G protein-coupled receptor binding, and more were among the enriched molecular functions.

Additionally, the GO cell components analysis yielded a remarkable enrichment of 189 entries ($P < 0.05$), mainly focusing on cellular membranes, extracellular regions, immunoglobulin complexes, vesicles, and secretory granules. These cellular components play essential roles in immune response, cytokine secretion, and intercellular signal transduction processes.

The findings from the GO enrichment analysis strongly suggest that the differentially expressed genes between the NHIC and HIC groups are critical players in immune response and regulation. These genes likely play pivotal roles in the underlying mechanisms contributing to the pathogenesis of both groups, shedding light on the intricate and complex nature of bladder disorders like BPS/IC. The insights gained from this analysis

may pave the way for further investigations and potential therapeutic strategies targeting the immune-related pathways implicated in these conditions.

GSEA analysis of NHIC and HIC bladder tissue

Our Gene Set Enrichment Analysis (GSEA) of KEGG Pathways yielded insightful results, with a total of 326 pathways identified, out of which 177 exhibited significant enrichment. Among these pathways, our focus was primarily on those associated with infectious immunity, considering their potential relevance to the pathogenesis of the conditions.

Notably, in the HIC group, several pathways related to viral infections were significantly upregulated, including Epstein-Barr virus infection and human cytomegalovirus infection. Additionally, pathways linked to bacterial infections such as pathogenic Escherichia coli infection and Staphylococcus aureus infection showed significant upregulation. Furthermore, key immune response-related pathways, such as cytokine-cytokine receptor interactions, antigen processing and presentation, natural killer cell-mediated cytotoxicity, T cell receptor signaling pathway, and B-cell receptor signaling pathway, were also found to be upregulated in the HIC group.

In contrast, several pathways related to metabolism exhibited significant downregulation in the HIC group. These pathways included cytochrome P450 metabolism of heterogeneous substances, oxidative phosphorylation, retinol metabolism, butyrate metabolism, glycine, serine, and threonine metabolism, steroid hormone biosynthesis, valine, leucine, and isoleucine degradation, pentose and glucuronic acid interconversion, glutathione metabolism, PPAR signaling pathway, fatty acid metabolism, phenylalanine metabolism, peroxisome, tyrosine metabolism, fatty acid degradation, glyoxylic acid and dicarboxylic acid metabolism, carbon metabolism, porphyrin metabolism, propionate metabolism, arachidonic acid metabolism, cysteine and methionine metabolism, fat digestion and absorption, bile secretion, and more.

To better understand the pathways relevant to the pathogenesis, we visualized the significant pathways in Fig. 5, providing a comprehensive overview of the molecular processes that may contribute to the development and progression of HIC.

Multi-omics integration analysis

Integration of microbiome and metabolomics: a comprehensive analysis

In our study, we integrated metabolomics analysis and microbiota analysis by using the metabolite expression levels with significant differences between the NHIC and HIC groups as environmental factor data, and correlating them with the corresponding patient microbiota. This allowed us to construct a heat map illustrating the correlation between microbiota and metabolomics data. Specifically, Fig. 6A displays the correlation heat map for differential metabolites in positive ion mode, along with the corresponding patient microbiota, while Fig. 6C presents the correlation heat map for differential metabolites in negative ion mode, after matching the corresponding patient flora.

Integration of metabolomics and transcriptomics: unraveling molecular insights

Figure 6B portrays an analysis of the distinct and overlapping portions of the data between each group. In total, there are 19 pathways, with KEGG-enriched metabolic pathways in negative ion mode intersecting with those enriched by transcriptome KEGG, summing up to 23 pathways. Additionally, after intersecting the metabolic pathways and transcriptomes in positive and negative ion modes simultaneously, six pathways were identified, namely steroid hormone biosynthesis, glycine, serine, and threonine metabolism, neuroactive ligand receptor interaction, synaptic vesicle cycle, bile secretion, and metabolic pathway. Further, the positive ion mode and transcriptome intersection after enrichment revealed 13 unique metabolic pathways, including actin cytoskeleton regulation, arginine and proline metabolism, nicotine addiction, pancreatic secretion, cholinergic synapse, gastric acid secretion, sphingomyelin metabolism, insulin secretion, saliva secretion, cAMP signaling pathway, taste conduction, tryptophan metabolism, and glycerophospholipid metabolism. Likewise, the negative ion mode and transcriptome intersection and enrichment after enrichment yielded 17 unique metabolic pathways, namely thiamine metabolism, porphyrin metabolism, fatty acid biosynthesis, pantothenate and CoA biosynthesis, mineral absorption, glutathione metabolism, glyoxylic acid, and dicarboxylic acid metabolism, β-alanine metabolism, aminoacyl tRNA biosynthesis, lysine degradation, carbon metabolism, protein digestion and absorption, central carbon metabolism of cancer, pyrimidine metabolism, purine metabolism, amino acid biosynthesis, ABC transport, and other metabolic pathways.

Discussion

Previous research has documented that non-pregnant, healthy female vaginal microbiota are dominated by certain bacterial genera such as lactobacillus, actinomycetes, Prevosia, Weroncoccus, Streptococcus, Proteus, Bacteroides, and Burkholderia[9]. Among these, lactobacillus is the most abundant genus, thriving in anaerobic conditions within the vaginal environment. It is capable of producing lactic acid, hydrogen peroxide, bacteriocins, and other antimicrobial agents, which help to prevent the invasion of foreign pathogens and to maintain a healthy microbiome within the vagina[9]. In contrast, Gardnerella is the most common genus associated with bacterial vaginosis in women, and Trichomonas vaginalis, a species of Gardnerella, has virulence factors that enable it to adhere to epithelial cells, forming biofilm communities that give it a competitive advantage over Lactobacillus[10]. Klebsiella, a pathogen found commonly in healthy individuals within the nose, throat, skin, and intestines, can cause a range of infections such as pneumonia, surgical wound infections, urinary tract infections, and sepsis[11]. Prevotella is a common dominant bacterium found in the oral cavity and is linked to various diseases such as inflammatory autoimmune disorders, opportunistic infections, bacterial vaginosis, and oral biofilm formation. As a common intestinal flora, it is also involved in the regulation of the intestinal inflammatory response[12].

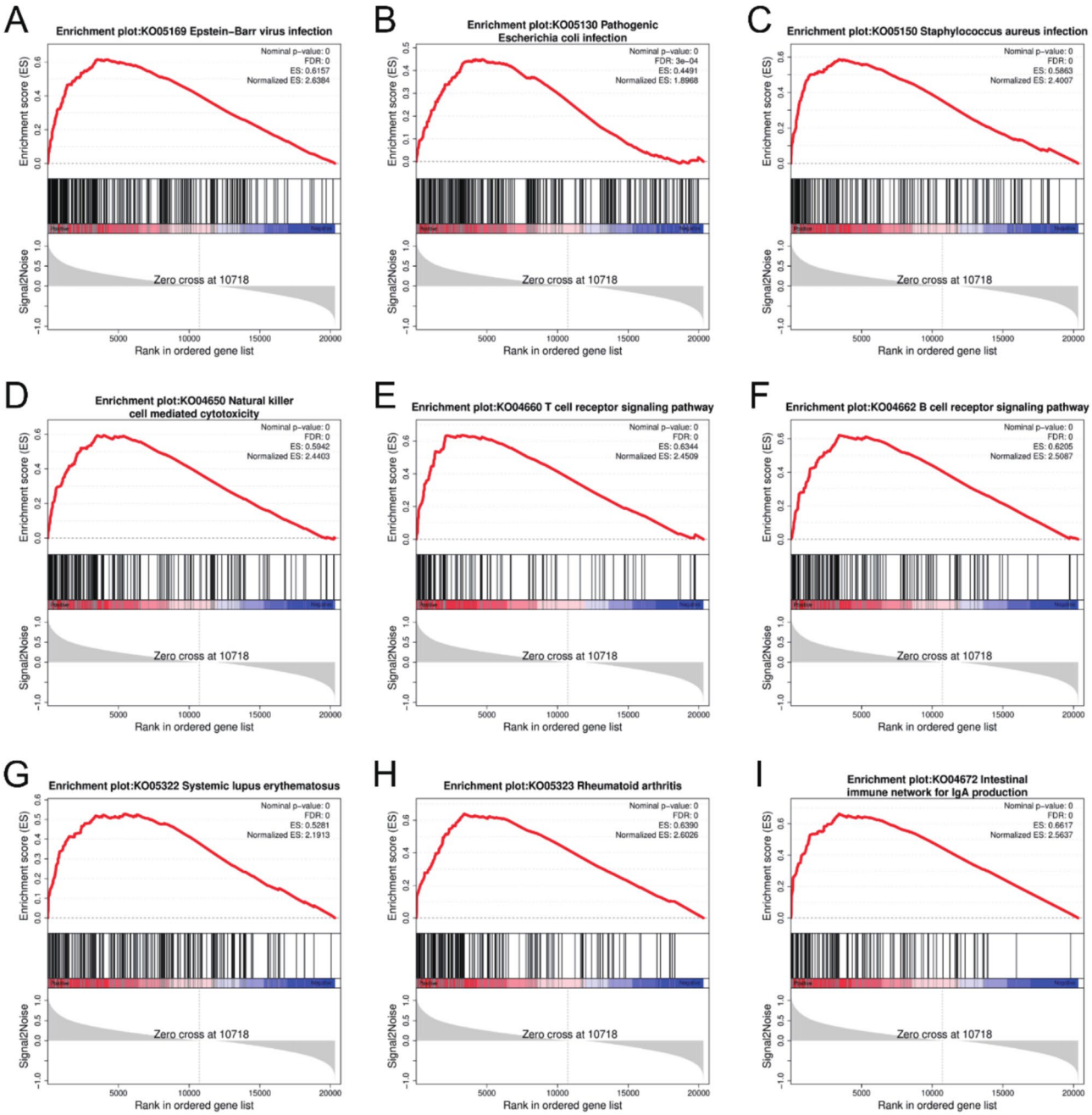

Fig. 5. GSEA (Gene Set Enrichment Analysis) analysis of the NHIC and HIC transcriptomic profiles.

Cardos allogeneis is a rare cause of urinary tract infection, and its association with the disease is unclear[13]. The Staphylococcus genus is found on human skin and mucous membranes, with Staphylococcus aureus and Staphylococcus epidermidis being common pathogens[14]. Vengoldia macrofungalis is a conditionally pathogenic bacterium associated with nosocomial device infections[15]. Streptococcus species are found as physiological flora in the human mouth and intestines, and some of these streptococci can cause opportunistic infections when human immunity is compromised[16]. Enterococci are common microbiota in the human gut microbiota and are also common pathogens causing urinary tract infections, soft tissue infections, and medical device infections[17]. The Paracoccus genus is taxonomically diverse, with more than 80 newly isolated species from various primitive and contaminated environments. These spherical gram-negative bacteria have diverse metabolic properties, which are useful for bioplastic synthesis and biodegradation[18]. Bacterium aquaticus is commonly found in soil and freshwater environments[19,20].

Our analysis of the microflora present in catheterized urine samples and self-retained mid-morning urine samples revealed no significant differences in the α diversity and β diversity indices, indicating similar richness and evenness of bacterial species in both groups. Furthermore, our comparison of the NMDS analysis between the two groups indicated that the MID group encompassed the CATH group, suggesting that the midstream

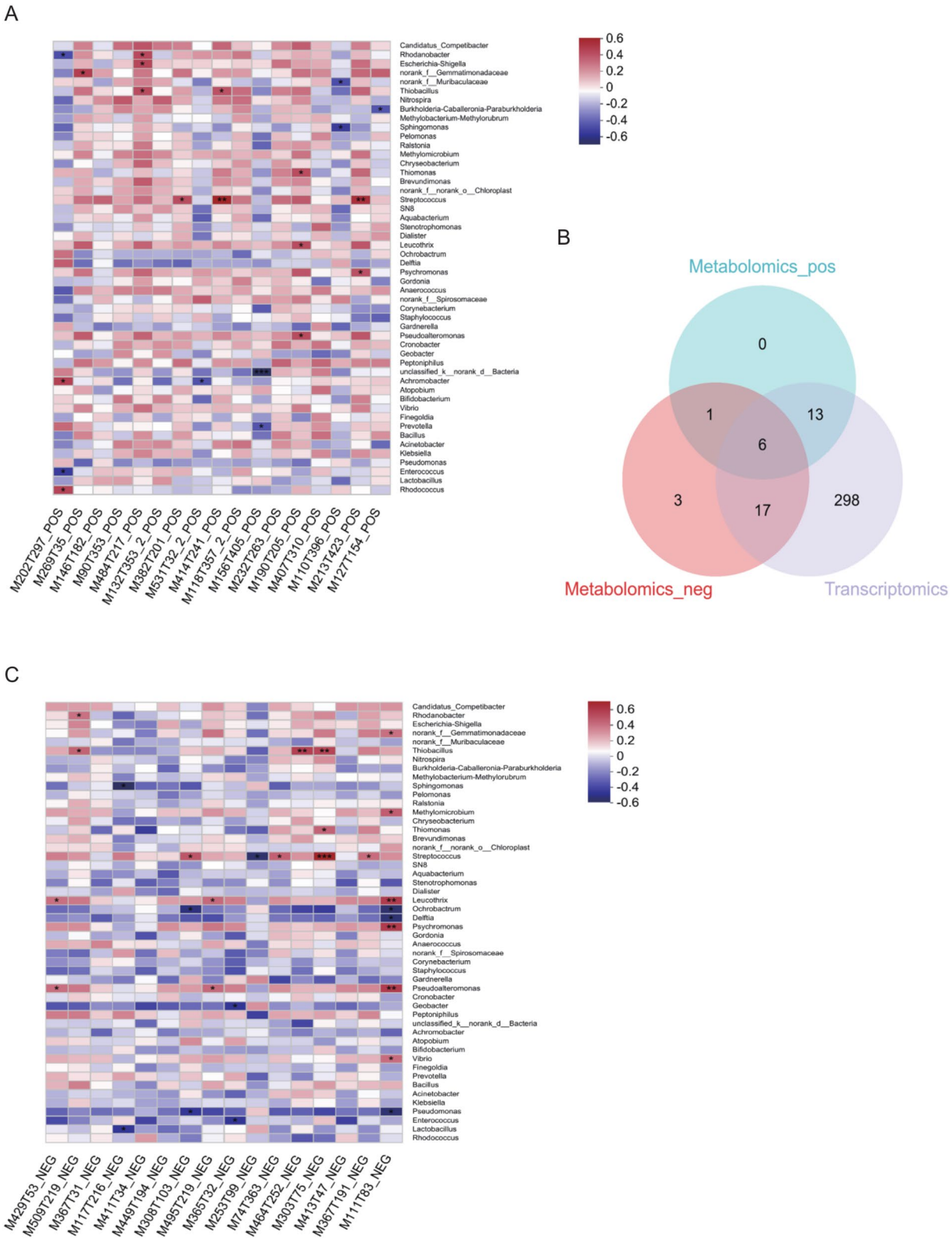

Fig. 6. Multi-omics Integration Analysis (**A**) Heatmap depicting the correlation between differential metabolites in the positive ion mode and microbial community in the NHIC and HIC groups; (**B**) Venn diagram depicting the overlapping KEGG enrichment pathways between the metabolomic and transcriptomic datasets; (**C**) Heatmap illustrating the correlation between differential metabolites in the negative ion mode and the microbial community in the NHIC and HIC groups.

urine collected by the patient contained a broader range of bacterial species and also implying that catheterization could exclude some bacterial species from the sample.

We further analyzed the dominant microbial communities in both groups and found that the MID group had a predominance of beneficial vaginal resident bacteria such as Lactobacillus, as well as common gut bacteria like Prevotella, Streptococcus, and Proteus. Additionally, there were various pathogenic bacteria present, including Staphylococcus, Klebsiella, and Cardos allogeneis, which are commonly associated with infections. In the MID group, there were also common environmental bacteria such as Streptococcus and Pseudomonas, which were typically found in water and soil. This suggested that midstream urine samples collected by patients were more susceptible to contamination from vaginal microbiota, gut microbiota, and environmental microbiota. The CATH group, on the other hand, had a higher proportion of Pseudomonas, which was a common pathogenic bacterium in hospital-acquired infections. This highlighted the importance of strict aseptic techniques during catheterization to prevent sample contamination from these bacteria.

NHIC and HIC, being two subtypes of a disease, share a plethora of similarities. In terms of urine microbiota analysis, although there exist minor distinctions in the α and β diversity, they are not statistically significant, thereby rendering urine flora alone insufficient to distinguish between the two groups. A prior research study, encompassing 21 women with HIC and 22 women with NHIC, also attests to the lack of marked differences in species abundance between HIC and NHIC patients. This observation displayed the current dearth of unique pathogenic microbiota, enabling to differentiate NHIC from HIC[5].

Our investigation has also established that while there is no significant variation in species abundance and evenness in the urine microbiota between NHIC and HIC patients, their dominant flora types differ considerably. The NHIC group presented with a clear preponderance of Lactobacillus, Klebsiella, Enterococcus, Staphylococcus, and Prevosia, whereas the HIC group had a marked predominance of Pseudomonas and Gardnerella. Using the Lefse multi-level species discrimination analysis, we discovered that the Proteus genus was significantly enriched in the HIC group, while the Digestive Coccus genus was significantly enriched in the NHIC group, thus displaying significant distinctions between the two groups. Proteus mirabilis and Proteus vulgaris of the Proteus genus are common opportunistic pathogenic bacteria that induce urinary tract infections by utilizing urease to decompose urea nitrogen, increase urine pH, and by invading and colonizing the host urinary tract through various virulence factors such as urease, stone formation, fimbriae and other adhesions, iron and zinc acquisition, protease and toxin, biofilm formation, and pathological mechanism regulation. Literature has also demonstrated a correlation between the increase of Proteus and inflammatory bowel disease. Digestive coccus is a normal flora present widely in the mouth, intestines, female reproductive tract, and skin, and is a gram-positive obligate anaerobic bacterium that can result in bacteremia and various purulent infections in the human body under pathogenic circumstances. The dissimilarities in dominant flora composition and the differences in enriched flora between the two groups imply dissimilarities in pathogenesis.

In our transcriptome differential gene analysis, we observed a significant upregulation of IL1β, IL6R, CCL3, TGFβR1, NGFR, and other genes in the HIC group, which are involved in the signal transduction mechanism of mast cell degranulation[21]. These findings led us to postulate that the inflammatory response associated with the HIC group may be closely linked to mast cells. Moreover, we found that pathways related to pathogen infections such as cytomegalovirus and Epstein-Barr virus, as well as bacterial infections including Escherichia coli and Staphylococcus aureus, were significantly upregulated in the HIC group. Similarly, pathways related to rheumatoid immune diseases like rheumatoid arthritis, systemic lupus erythematosus, autoimmune thyroid disease, and inflammatory bowel disease were also upregulated in this group, suggesting that HIC patients may have a history of recurrent bacterial and viral infections that caused abnormal autoimmune mechanisms, resulting in the development and progression of the disease. Previous literature has also reported multiple/frequent rheumatic immune diseases such as systemic lupus erythematosus, rheumatoid arthritis, Sjogren's syndrome, and inflammatory bowel disease[22–25], indicating that BPS/IC may be immune-related inflammation caused by autoimmune dysfunction, and this autoimmune mechanism link is more prominent in patients with HIC in our study. Conversely, in the NHIC group, we observed significant upregulation of various metabolic pathways such as amino acids, fatty acids, carbon metabolism, and oxidative phosphorylation, which suggests that NHIC patients may have nutritional metabolism disorders that contribute to the development and progression of the disease.

Previous studies investigating BPS/IC, when combined with normal control group urine flora and metabolome analysis, have found that the expression of Serratia, Brachybacter, Porphyromonas, and Citherobacterium was upregulated in the BPS/IC group. The metabolic pathways associated with sphingosine metabolism, fatty acid biosynthesis, and amino acid metabolism in the BPS/IC group were also significantly different from those in the control group. These studies have suggested that an increase in plant sphingosine and S1p may be related to BPS/IC symptoms mediated by bladder mast cell activation[6]. However, to date, no studies have been found that investigate the microbiome combined with metabolomic analysis associated with the two subtypes of HIC.

These findings suggest that there may be a relationship between the altered microbiome and metabolic pathways in HIC and NHIC. The negative correlations between specific bacteria and metabolites may indicate potential mechanisms underlying the pathogenesis of the disease. For example, the negative correlation between Prevobacterium and histidine suggests that the metabolism of this amino acid may be affected in NHIC patients. Similarly, the negative correlation between Pseudomonas and uracil and 5′-acetyladenosine suggests that this bacterium may affect nucleotide metabolism in HIC patients. These findings provide a starting point for further research into the metabolic pathways involved in the pathogenesis of HIC and NHIC.

The downregulation of actin cytoskeleton-related pathways in the HIC group may indeed contribute to bladder contractile dysfunction in patients with ICH. Actin cytoskeleton plays an essential role in regulating the contraction and relaxation of smooth muscle cells in the bladder wall. The contraction of smooth muscle cells is primarily driven by the interaction between actin and myosin filaments. The actin cytoskeleton provides

a structural framework for the formation of stress fibers, which generate tension to drive bladder contraction. The downregulation of actin cytoskeleton-related pathways may result in the destabilization of stress fibers and impair the contraction of smooth muscle cells, leading to bladder dysfunction. Additionally, the downregulation of insulin secretion and pyrimidine and purine metabolism pathways in the HIC group may also contribute to bladder dysfunction, as these pathways are involved in regulating smooth muscle cell contraction and relaxation. Insulin regulates bladder smooth muscle cell contractility by modulating the activity of potassium channels, which are crucial for maintaining the membrane potential of smooth muscle cells. Pyrimidine and purine metabolism pathways are also involved in regulating smooth muscle cell contraction by modulating the availability of intracellular calcium, which is a key mediator of smooth muscle cell contraction.

We undertook a comprehensive review of domestic and foreign literature on differential metabolites and enriched metabolic pathways to further elucidate the intricate interplay between the functions of differential microbiota, metabolites, and metabolic pathways enriched by differential genes and diseases. Histidine, an essential amino acid, is synthesized via the action of histamine decarboxylase. Mast cells store histamine in their granules and release histamine primarily through IgE-dependent degranulation.

Histamine mainly induces allergic reactions and inflammation via H1 and H4 receptors and participates in and regulates the immune response primarily through H1, H2, and H4 receptors[26]. Previous studies have confirmed that mast cell degranulation releases histamine in the inflammatory response of interstitial cystitis[27]. Through multi-omics joint analysis, we can infer that changes in histidine levels in NHIC patient urine can regulate mast cell degranulation and histamine release, potentially contributing to the different pathogenesis of NHIC and HIC phenotypes.

Benedikte Richter[28] found that YKL-40 and mast cells are associated with detrusor fibrosis and can be used to assess bladder fibrosis. HIC patients exhibit lower bladder capacity and more severe bladder fibrosis, indirectly suggesting that mast cells may be involved in the progression of HIC. This is consistent with our research findings.

However, in recent years, there has been an increasing focus on immune-related hypotheses, suggesting that mast cells may not play a central role in the pathogenesis of HIC. Yoshiyuki Akiyama and colleagues[29] conducted transcriptomic analyses of Hunner lesions and non-lesion areas, finding no significant differences in lymphoplasmacytic and mast cell infiltration or the CD4/CD8 T lymphocyte ratio. Robert M. Moldwin and colleagues[30] confirmed through immunohistochemistry that the activation of B cells and plasma cells is associated with the disease state of HIC. However, their study design could not determine whether the presence of these cells is a cause or a result of the disease. Kwang Jin Ko and colleagues[31] proposed that, compared to non-Hunner lesions, Hunner lesions exhibit reduced expression of anti-inflammatory and immunosuppressive factors, along with changes in immune cell populations. They suggested that macrophage polarization might be involved in the progression from non-Hunner lesions to Hunner lesions.

Based on a comprehensive review of various studies, the mechanisms underlying HIC remain complex and diverse. Mast cells and immune cells may play distinct roles at different stages of the disease or in different patient subgroups. Furthermore, the pathological characteristics of HIC may vary among individuals, which could also explain the discrepancies in research findings.

β-Hydroxy-β-methylbutyrate, a metabolite of leucine in essential amino acids, can stimulate protein synthesis by upregulating the mTOR pathway and anabolic signaling pathways such as growth hormone. This compound can also reduce proteolysis by downregulating catabolic signaling pathways such as ubiquitin proteasome and autophagic lysosomal system. This has significant implications for muscle damage repair, as β-hydroxy-β-methylbutyrate has been shown to be effective in treating various cachexia forms of muscle wasting in in vitro experiments[32]. NHIC patients had a higher abundance of lactobacilli than HIC patients, and lactobacillus was significantly negatively correlated with β-hydroxy-β-methylbutyrate. This observation suggests that protein synthesis was reduced, and the muscle injury repair pathway was not active in NHIC patients.

Uracil is a base specific to RNA. Recently, it has been found that the misbinding of cytosine deamination or DNA replication deoxyuridine 5′-triphosphate nucleotide (dUTP) leads to uracil in DNA. This compound has a barrier against infectious pathogens and is both a factor in antibody diversification in adaptive immunity and an effective antiviral drug[33]. Uridine, an endogenous small molecule metabolite composed of uracil and ribose, is involved in the synthesis of biofilms and RNA, which is of great significance for cell growth and function. In the environment of ischemia and hypoxia, uridine can increase lipid and glucose metabolism and prevent cell necrosis[34]. Our study revealed that Pseudomonas in HIC patients were the dominant bacteria and were significantly negatively correlated with uracil. We speculate that Pseudomonas may be involved in regulating pyrimidine metabolism, thereby mediating the necrosis of bladder urothelial cells and the occurrence of bladder wall ulcers.

Our study has certain limitations. Due to the challenges in sample collection, the final sample size included in the study was relatively small. In future research, we plan to improve the collection process and expand the sample size for further analysis. Additionally, this study only included a disease group and lacked a healthy control group. For urine collection, we used catheterized urine sampling, which is more precise for microbiome and metabolomics analysis compared to midstream morning urine. However, transcriptomic analysis also required bladder biopsy tissues, which are invasive procedures and not feasible for healthy individuals. As a result, we did not include a healthy control group in this study, making it impossible to determine whether the observed differences are disease-specific. In future studies, our research team will continue to refine the methodology and further explore the differences between disease and healthy control groups.

Conclusion

The pathogenesis of NHIC and HIC is still enigmatic, and further fundamental experiments are necessary to confirm the findings. However, the information gleaned from bioinformatics analysis provides a crucial stepping stone towards comprehending the underlying mechanisms of the two phenotypes.

Through the application of multi-omics analysis, we have established that NHIC and HIC exhibit notable differences in their microbiome, metabolomics, and transcriptomics, thereby indicating that the pathogenesis of these two types is distinct. Specifically, our examination revealed significant variances in the Proteus and peptic genera in the NHIC group, although further inquiry is warranted to ascertain whether these genera can be utilized as markers for distinguishing between the two types. Our transcriptome difference analysis unveiled that the upregulation of inflammation-related genes in the HIC group is closely linked to the mast cell degranulation transduction mechanism. Additionally, bacterial viral infection and rheumatic immune disease-related pathways were considerably upregulated in the HIC group, thereby signifying that individuals with HIC may have suffered from repeated bacterial viral infections in the past, causing an aberration in their autoimmune mechanism, which led to the development and manifestation of the disease. With regards to metabolic pathways, several nutrient and energy consumption-related processes were significantly upregulated in the NHIC group, thereby suggesting that these patients may have nutrient and energy metabolism disorders that contribute to the development of the disease. Our metabolome combined transcriptome analysis also indicated that bladder systolic dysfunction in HIC patients could be related to the downregulation of actin cytoskeleton-related pathways. Through our multi-omics joint analysis, we have inferred that Prévobacterium species, which is advantageous in the urine of NHIC patients, may regulate the inflammatory response by altering histidine changes, which could affect mast cell degranulation and histamine release. Furthermore, the dominant bacterium Lactobacillus may negatively regulate β-hydroxy-β-methylbutyrate, which is implicated in the damage and repair mechanism of muscle. In contrast, Pseudomonas, which is significantly dominant in the urine of HIC patients, could be involved in regulating pyrimidine metabolism, lipid, and glucose metabolism, thereby mediating the necrosis of bladder urothelial cells and the formation of bladder wall ulcers. It is important to note that these are only preliminary inferences, as the occurrence and development of a disease is a complex interplay between genetics, environment, and other factors.

Methods

Ethical declaration and informed consent

The proposal of this research project has been approved by the Ethics Committee of Peking University People's Hospital and is in line with the provisions of the Declaration of Helsinki. The ethical approval number is 2022PHB400-001. All patients signed informed consent.

Specimen acquisition

The specimen repository compiled bladder tissue samples from two cohorts of NHIC and HIC patients who underwent cystoscopy with hydrodilation surgery. HIC is a type of pancystitis[35], therefore, during the biopsy procedure, we collected two samples from the Hunner lesion and one sample each from the surrounding mucosa (upper, lower, left, and right), for a total of six points. After the surgeon extracted the bladder tissue samples, the laboratory personnel immediately performed liquid nitrogen flash freezing. The samples were then transported to a liquid nitrogen tank and, once a sufficient number of samples were collected, they were shipped on dry ice for further processing.

Urine samples were collected via two different retention methods: surgeon-retained urine before surgery and early mid-morning urine specimens retained by the patients before surgery. The patients' self-retained mid-morning urine sample was categorized as the MID group, while the intraoperative catheterization sample was designated as the CATH group.

The urine samples collected from patients were transported to the laboratory, where they were centrifuged at 3000 rpm for 10 min at 4 °C. The clear supernatant was then aliquoted into centrifuge tubes, with 1.5 ml per tube. Four tubes were prepared for each sample: two for urine microbiome analysis and two for metabolomics analysis. After proper labeling, the samples were flash-frozen in liquid nitrogen for 15 min and stored in a − 80 °C freezer. Once a sufficient number of samples were collected, they were shipped on dry ice for further processing.

DNA extraction and PCR amplification: Total microbial genomic DNA was extracted from urine samples using FastDNA® Spin Kit for Soil (MP Biomedicals, U.S.) according to manufacturer's instructions. The quality and concentration of DNA were determined by 1.0% agarose gel electrophoresis and a NanoDrop2000 spectrophotometer (Thermo Scientific, United States) and kept at − 80 ℃ prior to further use. The hypervariable region V3-V4 of the bacterial 16S rRNA gene were amplified with primer pairs 338F (5′-ACTCCTACGGGAGG CAGCAG-3′) and 806R(5′-GGACTACHVGGGTWTCTAAT-3′)[36] byT100 Thermal Cycler PCR thermocycler (BIO-RAD, USA). The PCR reaction mixture including 4 μL 5 × Fast Pfu buffer, 2 μL 2.5 mM dNTPs, 0.8 μL each primer (5 μM), 0.4 μL Fast Pfu polymerase, 0.2uL BSA, 10 ng of template DNA, and ddH2O to a final volume of 20 μL. PCR amplification cycling conditions were as follows: initial denaturation at 95 ℃ for 3 min, followed by 29 cycles of denaturing at 95 ℃ for 30 s, annealing at 53 ℃ for 30 s and extension at 72 ℃for 45 s, and single extension at 72 ℃ for 10 min, and end at 10 ℃. The PCR product was extracted from 2% agarose gel and purified using the PCR Clean-Up Kit (YuHua, Shanghai, China) according to manufacturer's instructions and quantified using Qubit 4.0 (Thermo Fisher Scientific, USA) .

Extraction of urine metabolites was performed using the methanol/acetonitrile extraction method. After the samples were slowly thawed at 4 °C, 100 μL of each sample was taken and mixed with 400 μL of pre-cooled methanol/acetonitrile solution (1:1, v/v). The mixture was vortexed and left to stand at − 20 °C for 30 min, followed by centrifugation at 14,000*g* for 20 min at 4 °C. The supernatant was collected and vacuum-dried. For mass spectrometry analysis, the dried metabolites were reconstituted in 100 μL of acetonitrile–water solution (acetonitrile:water, 1:1, v/v), vortexed, and centrifuged again at 14,000*g* for 15 min at 4 °C. The resulting supernatant was used for sample injection and analysis.

Approaches for investigating the urinary microbiome

Genomic DNA is first extracted from the sample, and the conserved region of rDNA is amplified using specific primers with barcodes. The PCR amplification products are then quantified and purified before being combined in equal amounts to construct a sequencing library. Illumina PE250 sequencing is then performed on the library, and the resulting raw reads are filtered to eliminate low-quality sequences. The remaining high-quality reads are assembled and stitched into tags, which are then filtered, resulting in clean tags. The clean tags are used for clustering based on UPARSE algorithm, and the resulting effective tags are analyzed for OTU abundance statistics. The processed data is then subjected to species annotation, α diversity analysis, β diversity analysis, community function prediction, and other analyses. If valid groupings exist, between-group comparisons and statistical tests are performed. Finally, more advanced analyses such as CCA are conducted in conjunction with other factors, such as environmental factors or metabolomics results, to answer questions regarding the relationship between microbes and the environment.

Approaches for urinary metabolomics analysis

Following sample collection, specimens undergo rigorous quality control, screening, and subsequent formal experimentation and bioinformatics analysis. During experimental procedures, a combination of positive and negative ion modes (POS and NEG, respectively) is employed, allowing for enhanced coverage and more robust detection results. In the subsequent data analysis phase, separate analyses of positive and negative ion modes are performed.

Qualitative and quantitative analysis of metabolites

Non-targeted metabolomics utilizes high-resolution mass spectrometry (HRMS) detection technology to detect as many molecular characteristic peaks in the sample as possible. The technique combines public databases such as Mass Bank, Metlin, MoNA, and self-built secondary mass spectrometry databases for substance annotation.

Differential metabolite identification and analysis

We integrated multivariate statistical analysis of the VIP value of OPLS-DA and univariate statistical analysis using T-test *P* value to screen for differential metabolites across various comparison groups. The set threshold for differential significance was: VIP ≥ 1 and T-test $P < 0.05$ in the OPLS-DA model. The VIP plot of OPLS-DA is employed to showcase the significance of variables and their contribution towards sample differentiation.

Metabolic pathway analysis

Following the identification of differential metabolites, we performed KEGG enrichment analysis to determine the key biochemical metabolic pathways and signal transduction pathways that were impacted by these metabolites across groups.

Liquid chromatography-mass spectrometry analysis

Liquid chromatography-mass spectrometry (LC–MS/MS) analysis was performed using an Agilent 1290 Infinity LC system coupled to a SCIEX TripleTOF 6600 mass spectrometer. Chromatographic separation was achieved on a Waters ACQUITY UPLC BEH Amide column (1.7 μm, 2.1 × 100 mm) maintained at 25 °C. The mobile phase consisted of (A) 25 mM ammonium acetate/25 mM ammonium hydroxide in water and (B) acetonitrile, delivered at 0.5 mL/min with the following gradient: 95% B (0–0.5 min), linear reduction to 65% B (0.5–7 min), further reduction to 40% B (7–8 min), isocratic hold (8–9 min), and re-equilibration at 95% B (9.1–12 min). Electrospray ionization operated at ± 5500 V with source gases set to 60 psi (Gas1 and Gas2) and 30 psi curtain gas, at 600 °C source temperature. Full-scan MS data (m/z 60–1000) and data-dependent MS/MS scans (m/z 25–1000) were acquired in high-sensitivity mode using information-dependent acquisition (IDA) with collision energy of 35 ± 15 eV and declustering potential of ± 60 V. Quality control samples (pooled from all specimens) were injected every 10 samples to monitor system stability (retention time RSD < 0.1 min; intensity RSD < 15%). Raw data were converted to .mzML format (ProteoWizard v3.0.6428), processed using XCMS Online (v3.7.1) with centWave peak detection (m/z tolerance = 10 ppm; peak width = 10–60 s), and normalized to total peak area after filtering features with > 50% missingness within experimental groups.

Transcriptomic research methods of bladder biopsy

After collecting tissue samples, RNA extraction was conducted using the Trizol reagent kit (Invitrogen, Carlsbad, CA, USA), according to the manufacturer's instructions. Agilent 2100 Bioanalyzer (Agilent Technologies, Palo Alto, CA, USA) was used to assess RNA quality. The total RNA extraction was followed by the enrichment of eukaryotic mRNA using Oligo(dT). Subsequently, the enriched mRNA underwent fragmentation using a fragmentation buffer, followed by reverse transcription into cDNA utilizing the NEBNext Ultra RNA Library Prep Kit for Illumina (NEB#7530, New England Biolabs, Ipswich, MA, USA). The resulting library was subjected to sequencing on an Illumina Novaseq6000 platform by Gene Denovo Biotechnology Co. (Guangzhou, China).

After ribosomal RNA was aligned, the genome alignment was performed using HISAT2[37], and quantification was conducted based on StringTie[38]. The FPKM values were calculated using RSEM (v1.3.3, URL: https://github.com/deweylab/RSEM/archive/v1.3.3.tar.gz) software. Differential analysis between groups was performed using DESeq2(Fold change ≥ 2 and FDR < 0.05). Geneontology (GO) and Kyoto Encyclopedia of Genes and Genomes[39–41] (KEGG) enrichment analyses of DEmRNAs were performed using hypergeometric Tests.

Additionally, gene set enrichment analysis (GSEA) was used for the elucidation of the function of differentially expressed genes between groups.

Integrated analysis

Statistical analysis and visualization in this study were conducted using R software (version 3.6.3).

Integration of metabolomics and microbiome analysis

Significant differences in metabolite expression between the NHIC and HIC groups in metabolomics analysis were used as environmental factor data and matched with the corresponding patient's microbiome analysis. This allowed for the generation of a correlation heat map for the integration of microbiome and metabolomics analysis.

Integration of metabolomics and transcriptomics analysis

We analyzed the unique and shared portions of the data between each group and visualized the results using the ggplot2 and VennDiagram packages. The intersection of metabolite pathways enriched by KEGG analysis in positive and negative ion modes with pathways enriched by transcriptomics analysis yielded the shared pathways.

Data availability

The raw sequence data reported in this paper have been deposited in the Genome Sequence Archive (Genomics, Proteomics & Bioinformatics 2021) in National Genomics Data Center (Nucleic Acids Res 2022), China National Center for Bioinformation/Beijing Institute of Genomics, Chinese Academy of Sciences (GSA-Human: HRA012042) that are publicly accessible at https://ngdc.cncb.ac.cn/gsa-human.

Received: 23 December 2024; Accepted: 14 July 2025
Published online: 22 July 2025

References

1. Malde, S., Palmisani, S., Al-Kaisy, A. & Sahai, A. Guideline of guidelines: Bladder pain syndrome. *BJU Int.* **122**, 729–743 (2018).
2. Fall, M., Johansson, S. L. & Aldenborg, F. Chronic interstitial cystitis: A heterogeneous syndrome. *J. Urol.* **137**, 35–38 (1987).
3. Nickel, J. C. & Doiron, R. C. Hunner lesion interstitial cystitis: The bad, the good, and the unknown. *Eur. Urol.* **78**, e122–e124 (2020).
4. Walton, I. & Nickel, J. C. The urinary microbiome in interstitial cystitis/bladder pain syndrome? A critical look at the evidence. *J. Urol.* **206**, 1087–1090 (2021).
5. Nickel, J. C. et al. The bacterial microbiota of Hunner lesion interstitial cystitis/bladder pain syndrome. *BJU Int.* **129**, 104–112 (2022).
6. Xu, H. et al. Combined signature of the urinary microbiome and metabolome in patients with interstitial cystitis. *Front. Cell. Infect. Microbiol.* **11**, 711746 (2021).
7. Akiyama, Y. et al. Molecular taxonomy of interstitial cystitis/bladder pain syndrome based on whole transcriptome profiling by next-generation RNA sequencing of bladder mucosal biopsies. *J. Urol.* **202**, 290–300 (2019).
8. Zhu, L., Ke, H., Wang, Q. & Xu, K. Cystoscopy, an indispensable tool for the diagnosis and prognosis of bladder pain syndrome, takes nomograms for predicting recurrence. *World J. Urol.* **41**, 2451–2458 (2023).
9. Aagaard, K. et al. A metagenomic approach to characterization of the vaginal microbiome signature in pregnancy. *PLoS ONE* **7**, e36466 (2012).
10. Schwebke, J. R., Muzny, C. A. & Josey, W. E. Role of Gardnerella vaginalis in the pathogenesis of bacterial vaginosis: A conceptual model. *J. Infect. Dis.* **210**, 338–343 (2014).
11. Dong, N., Yang, X., Chan, E.W.-C., Zhang, R. & Chen, S. Klebsiella species: Taxonomy, hypervirulence and multidrug resistance. *EBioMedicine* **79**, 103998 (2022).
12. Tett, A., Pasolli, E., Masetti, G., Ercolini, D. & Segata, N. Prevotella diversity, niches and interactions with the human host. *Nat. Rev. Microbiol.* **19**, 585–599 (2021).
13. Klein, S. et al. Significant increase in cultivation of Gardnerella vaginalis, Alloscardovia omnicolens, Actinotignum schaalii, and Actinomyces spp. in urine samples with total laboratory automation. *Eur. J. Clin. Microbiol. Infect. Dis.* **37**, 1305–1311 (2018).
14. Paharik, A. E. & Horswill, A. R. The staphylococcal biofilm: Adhesins, regulation, and host response. *Microbiol. Spectr.* **4**, 2016.
15. Brüggemann, H. et al. Pan-genome analysis of the genus Finegoldia identifies two distinct clades, strain-specific heterogeneity, and putative virulence factors. *Sci. Rep.* **8**, 266 (2018).
16. Krzyściak, W., Pluskwa, K. K., Jurczak, A. & Kościelniak, D. The pathogenicity of the Streptococcus genus. *Eur. J. Clin. Microbiol. Infect. Dis.* **32**, 1361–1376 (2013).
17. García-Solache, M. & Rice, L. B. The Enterococcus: A model of adaptability to its environment. *Clin. Microbiol. Rev.* **32**, e00058-e118 (2019).
18. Puri, A., Bajaj, A., Singh, Y. & Lal, R. Harnessing taxonomically diverse and metabolically versatile genus *Paracoccus* for bioplastic synthesis and xenobiotic biodegradation. *J. Appl. Microbiol.* **132**, 4208–4224 (2022).
19. Sun, L., Chen, W., Huang, K., Lyu, W. & Gao, X. Aquabacterium soli sp. nov., a novel bacterium isolated from soil under the long-term application of bifenthrin. *Int. J. Syst. Evol. Microbiol.* **71**, 004768 (2021).
20. Chen, W.-M., Chen, T.-Y., Kwon, S.-W. & Sheu, S.-Y. Aquabacterium lacunae sp. nov., isolated from a freshwater pond. *Int. J. Syst. Evol. Microbiol.* **70**, 2888–2895 (2020).
21. Metcalfe, D. D., Baram, D. & Mekori, Y. A. Mast cells. *Physiol. Rev.* **77**, 1033–1079 (1997).
22. Russell, A. L. Glycoaminoglycan (GAG) deficiency in protective barrier as an underlying, primary cause of ulcerative colitis, Crohn's disease interstitial cystitis and possibly Reiter's syndrome. *Med. Hypotheses* **52**, 297–301 (1999).
23. Kapoor, S. Beyond rheumatoid arthritis: The close association between interstitial cystitis and Sjogren's syndrome. *Neurourol. Urodynam.* **34**, 101–101 (2015).
24. de la Serna, A. R. & Alarcon-Segovia, D. Chronic interstitial cystitis as an initial major manifestation of systemic lupus erythematosus. *J. Rheumatol.* **8**, 808–810 (1981).
25. Vicencio, G. P., Chung-Park, M., Ricanati, E., Lee, K. N. & DeBaz, B. P. SLE with interstitial cystitis, reversible hydronephrosis and intestinal manifestations. *J. Rheumatol.* **16**, 250–251 (1989).
26. Hirasawa, N. Expression of histidine decarboxylase and its roles in inflammation. *IJMS* **20**, 376 (2019).
27. Lynes, W. L. et al. Mast cell involvement in interstitial cystitis. *J. Urol.* **138**, 746–752 (1987).
28. Lai, H. H., Pickersgill, N. A. & Vetter, J. M. Hunner lesion phenotype in interstitial cystitis/bladder pain syndrome: A systematic review and meta-analysis. *J. Urol.* **204**, 518–523 (2020).
29. Akiyama, Y. et al. Overexpression of HIF1α in Hunner lesions of interstitial cystitis: Pathophysiological implications. *J. Urol.* **207**, 635–646 (2022).
30. Moldwin, R. M. et al. Immune cell profiles of patients with interstitial cystitis/bladder pain syndrome. *J. Transl. Med.* **20**, 97 (2022).

31. Ko, K. J., Kim, G., Sung, H. H., Park, W.-Y. & Lee, K.-S. Potential role of macrophage polarization in the progression of Hunner-type interstitial cystitis. *Int. J. Mol. Sci.* **25**, 778 (2024).
32. Holeček, M. Beta-hydroxy-beta-methylbutyrate supplementation and skeletal muscle in healthy and muscle-wasting conditions. *J. Cachexia. Sarcopenia Muscle* **8**, 529–541 (2017).
33. Sire, J., Quérat, G., Esnault, C. & Priet, S. Uracil within DNA: An actor of antiviral immunity. *Retrovirology* **5**, 45 (2008).
34. Connolly, G. P. & Duley, J. A. Uridine and its nucleotides: Biological actions, therapeutic potentials. *Trends Pharmacol. Sci.* **20**, 218–225 (1999).
35. Maeda, D. et al. Hunner-type (Classic) interstitial cystitis: A distinct inflammatory disorder characterized by pancystitis, with frequent expansion of clonal b-cells and epithelial denudation. *PLoS ONE* **10**, e0143316 (2015).
36. Liu, C. et al. Denitrifying sulfide removal process on high-salinity wastewaters in the presence of Halomonas sp. *Appl Microbiol. Biotechnol.* **100**, 1421–1426 (2016).
37. Kim, D., Langmead, B. & Salzberg, S. L. HISAT: A fast spliced aligner with low memory requirements. *Nat. Methods* **12**, 357–360 (2015).
38. Pertea, M. et al. StringTie enables improved reconstruction of a transcriptome from RNA-seq reads. *Nat. Biotechnol.* **33**, 290–295 (2015).
39. Kanehisa, M., Furumichi, M., Sato, Y., Matsuura, Y. & Ishiguro-Watanabe, M. KEGG: Biological systems database as a model of the real world. *Nucleic Acids Res.* **53**, D672–D677. https://doi.org/10.1093/nar/gkae909 (2025).
40. Kanehisa, M. Toward understanding the origin and evolution of cellular organisms. *Protein Sci.* **28**, 1947–1951. https://doi.org/10.1002/pro.3715 (2019).
41. Kanehisa, M. & Goto, S. KEGG: Kyoto encyclopedia of genes and genomes. *Nucleic Acids Res.* **28**, 27–30 (2000).

Author contributions

Lin Zhu: Methodology, Investigation, Formal Analysis, Data Curation, Visualization, Writing—Original Draft. Hanwei Ke: Investigation, Visualization, Formal Analysis, Writing—Original Draft, Writing—Review & Editing. Qi Wang: Supervision, Validation. Kexin Xu: Conceptualization, Project Administration, Supervision, Funding Acquisition. Xiaofang Chen: Conceptualization, Supervision, Funding Acquisition.

Funding

This work was supported by the National Natural Science Foundation of China (81970660) and Beijing Natural Science Foundation (7242153).

Declarations

Competing interests

The authors declare no competing interests.

Ethics approval and consent to participate

This study was approved by the Medical Ethics Committee of Peking University People's Hospital (approval number: 2022PHB400-001). All procedures followed applicable guidelines and regulations. Informed written consent was also obtained from the patients in this study.

Consent for publication

All authors consent to the publication of this manuscript and declare no conficts of interest.

Additional information

Supplementary Information The online version contains supplementary material available at https://doi.org/10.1038/s41598-025-12010-w.

Correspondence and requests for materials should be addressed to K.X. or X.C.